J Mol Model (2003) 9:207–216
DOI 10.1007/s00894-003-0116-2

ORIGINAL PAPER

Alexandr V. Yatsenko

Molecular crystals: the crystal field effect on molecular electronic structure

Received: 31 October 2002 / Accepted: 10 December 2002 / Published online: 1 July 2003

Abstract The effect of crystal packing on the electronic structure of organic molecules was modeled by incorporation of the external electrostatic potential into the semiempirical Hamiltonian of the molecule. An empirical correction procedure was devised in order to compensate for systematic errors in the charge distribution typical of semiempirical methods. The model was applied to 79 crystal structures belonging to various syngonies and space groups. The effect of the crystal field is subject to wide variations depending on the crystal packing motif. The difference between the effect of the crystal field on the molecular electronic structure and the solvent effect modeled with COSMO is highlighted. The effect of intermolecular hydrogen bonds on the molecular electronic structure and electronic spectra was modeled with this approach, and it does not predominate over the effect of long-range electrostatic interactions. INDO/S calculations employing the crystal electrostatic potential give an insight into the origin of crystallochromy, in particular, they properly predict color difference for several groups of polymorphs. Supplementary material is available for this article if you access the article at http://dx.doi.org/10.1007/s00894-003-0116-2. A link in the frame on the left on that page takes you directly to the supplementary material.

Keywords Semiempirical methods · Dyes · Electrostatic potential · Polymorphism · Molecular crystals

Electronic Supplementary Material Supplementary material is available for this article if you access the article at http://dx.doi.org/10.1007/s00894-003-0116-2. A link in the frame on the left on that page takes you directly to the supplementary material.

A. V. Yatsenko (✉)
Department of Chemistry,
Moscow State University,
119992 Moscow, Russia
e-mail: yatsenko@biocryst.phys.msu.su

Introduction

Organic molecular crystals, films and aggregates are technologically very attractive materials. Their usefulness relies to a large extent on their light absorption and emission properties, photoconductivity, non-linear polarizability etc., i.e. the properties immediately related to the electronic structure of these materials. [1] A rigorous quantum mechanical treatment of a crystal requires determination of its band structure within periodic boundary conditions. Such calculations are very time consuming even for crystals built of medium-sized molecules, [2, 3] and thus several approximate models have been introduced in order to reduce the computational problem. One of the possible ways to do this is to restrict the quantum mechanical treatment to an individual molecule and to consider the intermolecular interactions in terms of the self-consistent reaction field. The molecular properties can be used further as input parameters in calculations of solid state properties, such as the energy of molecular packing or the band structure of the crystal at the level of exciton theory.

Beginning in the 1970s, several methods based on the incorporation of the external potential produced by the crystal environment of a molecule into its Hamiltonian have been introduced.[4, 5, 6, 7, 8, 9] These methods were then applied to molecular conformations, [10, 11, 12] crystal packing energies and UV–visible spectral shifts in crystals. [13, 14, 15]

The simplest methods of this group operate with a limited set (a few tens to a few hundreds) of point charges situated around the molecule of interest in order to mimic the effect of crystal environment. [5, 16] More sophisticated procedures involve the Ewald summation over the crystal lattice, taking into account atomic monopoles, dipoles, quadrupoles, etc. [6, 17] The technique for introducing the external field perturbation into the Hamiltonian has been devised in detail at various levels of theory. [6, 18, 19, 20] It is especially simple in the case of a semiempirical Hamiltonian of the NDO type or NDDO type: modification of the H_{core} matrix is restricted

to the diagonal elements and the one-atomic off-diagonals, whereas the diatomic terms remain unchanged. Thought not strict, this approach is widely used in the modeling of solvation effects.

It is obvious that the success of such a procedure depends on the accuracy of the representation of the molecular electrostatic potential (MEP), whereas the semiempirical schemes (especially NDO/S) are inferior to the correlation-corrected non-empirical methods (MP2 and DFT) in reproducing the electron density distribution and thus require empirical correction.

The following scheme [21] has been proposed for solving this problem:

1. The charge distribution in a molecule is modeled with the accurate semiempirical methods (AM1 and PM3).
2. The molecular charge distribution is corrected employing an empirical procedure [22] and then used to calculate the semiempirical crystal electrostatic potential (SCEP).
3. The potential thus obtained is introduced into the molecular Hamiltonian, and steps 1–3 are repeated until self-consistency is achieved.
4. The final potential can be introduced into a Hamiltonian of another type (e.g., INDO/S), but before doing that an additional empirical correction is necessary, in compensation for the systematic errors typical of this method.

When applied to three pairs of polymorphs, this scheme allowed explanation of their differences in color. Recently the performance of various semiempirical methods for dipole moments of a number of dye molecules has been examined. Using these results as a base, the methods of empirical correction have been improved, and the upgraded model was used to study the effect of crystal packing on molecular electronic structure in 79 crystal structures. The results are presented below.

Computational technique

Software used

The algorithm to be presented was implemented within the MOPAC7.2 [23] codes. In the previous work [21] it was shown that the effects of crystal field modeled with AM1 [24] and PM3 [25] agree well for all studied crystal structures. Since AM1 is a little bit more accurate than PM3 in reproducing the dipole moments of dye molecules, [22] in this study all SCEP calculations were performed with AM1. The INDO-CISD calculations with and without SCEP were run using the program provided by Dick [26, 27] with the Pariser–Parr formula [28] for the two-center Coulomb integrals and employing 300 energy-selected singles and doubles. The TD-DFT [29] calculations of excitations of isolated molecules were carried out with Gaussian 98 [30] using the standard 6-31G* basis set and the B3LYP [31, 32] hybrid exchange-correlation functional. This technique was found to be successful for a wide variety of dye molecules. [33] The AM1-CIS calculations were performed with HyperChem. [34]

Hamiltonian modification

In the NDDO approximation employing an *sp* basis, the MEP is formed by the contributions from atomic charges, dipoles and quadrupoles, since the higher multipole moments vanish by symmetry. [35] If a molecular crystal is formed only by the van der Waals interactions, the shortest intermolecular separations C...H and C...C are 2.8–2.9 Å and 3.3–3.4 Å, respectively. At the distances of this range, the contributions from atomic quadrupole moments make up a few percent of the total MEP; thus only atomic point charges and dipoles were used to calculate the crystal electrostatic potential.

The introduction of an external potential $V(r)$ into the molecular Hamiltonian gives rise to the following modification of the one-center core Hamiltonian elements:

$$H_{\mu\nu} = H^0_{\mu\nu} + \int \varphi^*_\mu(r) V(r) \varphi_\nu(r) \mathrm{d}r$$

Expanding $V(r)$ in a Taylor series up to the linear terms about the position of atom A the orbitals ϕ_μ and ϕ_ν are centered at, we obtain for diagonals:

$$H_{\mu\mu} = H^0_{\mu\mu} - V_A$$

and for one-center off-diagonals involving a $2s$ orbital and a $2p_{x(y,z)}$ orbital:

$$H_{\mu\nu} = H^0_{\mu\nu} - DD_A \cdot V'_A$$

where DD_A is the dipole charge separation [35] of an atom A, and all other terms of the H matrix remain unchanged.

These approximations fail if shorter intermolecular contacts, for example hydrogen bonds, are present in the crystal. In this case the intermolecular overlap also cannot be neglected. However, satisfactory results can be obtained by replacing the Coulomb potential with the potential defined by the Dewar–Sabelli–Klopman (DSK) formula [36, 37]

$$E(A,B) = \frac{q^A q^B}{\sqrt{R^2_{AB} + \frac{1}{4}\left(\frac{1}{\gamma^A} + \frac{1}{\gamma^B}\right)^2}},$$

where

$$\gamma = 1.0526 \times \gamma_{ss}(\mathrm{AM1})$$

In order to test this procedure, five compounds (Fig. 1) that adopt the pair arrangement in crystals (Figs. 2, 3, 4, 5, and 6) were used. Calculations at the AM1 level were carried out for isolated molecules, for molecular pairs explicitly, and for molecules under the potential (Coulomb and DSK) created by the second molecule of the pair. The results are shown in Table 1.

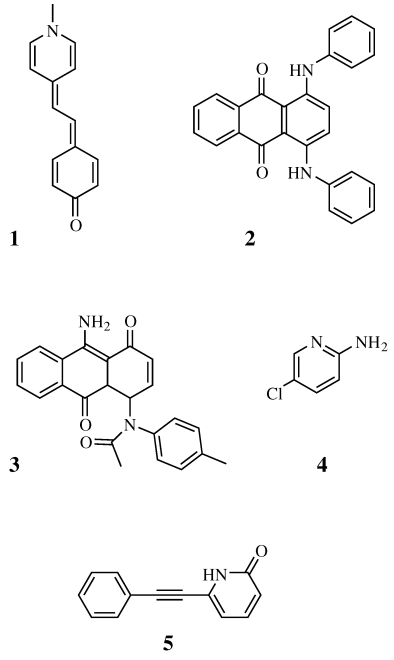

Fig. 1 Compounds used as test examples for the choice of potential (Table 1)

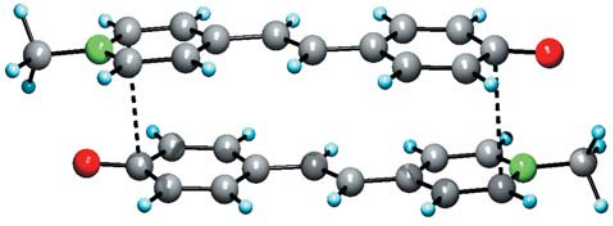

Fig. 2 Molecular pair in structure **1** (the shortest intermolecular C...C separation is 3.250 Å)

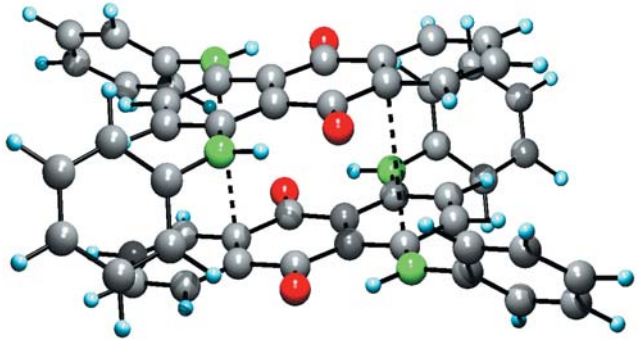

Fig. 3 Molecular pair in structure **2** (the shortest intermolecular C...C separation is 3.438 Å)

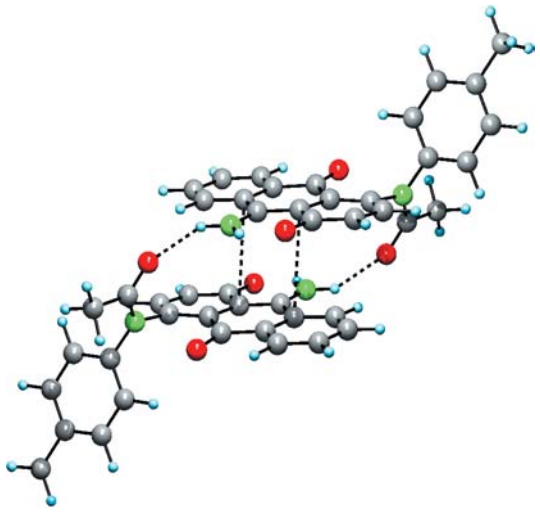

Fig. 4 Hydrogen-bonded molecular pair in structure **3** (the O...H distance is 2.06 Å; the shortest C...C separation is 3.464 Å)

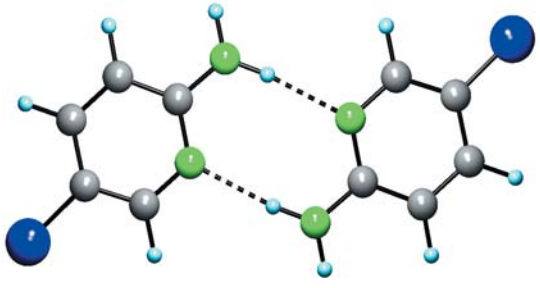

Fig. 5 Hydrogen-bonded molecular pair in structure **4** (the N...H distance is 2.06 Å)

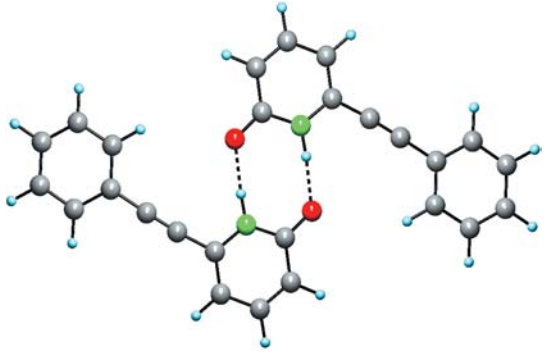

Fig. 6 Hydrogen-bonded molecular pair in structure **5** (the O...H distance is 1.79 Å)

For all five examples, the DSK formula reproduces the results obtained for molecular pairs better than the Coulomb potential. For structures **1** and **2**, where the intermolecular hydrogen bonds are absent, the results obtained with the DSK potential almost coincide with the results obtained for molecular pairs. If hydrogen bonds are present, as in structures **3**–**5**, the calculations with DSK overestimate their effect on the molecular dipole moment and charge distribution, but underestimate the change in the HOMO–LUMO energy gap. Thus, the proposed model could be quite a good approximation in

Table 1 Molecular dipole moments (μ), HOMO–LUMO gaps (ΔE), and average changes in atomic charges with respect to molecular dimers (Δq^{rms}) in **1**–**5** (Fig. 1)

Compound	μ (D)	ΔE (eV)	Δq^{rms} (e)[a]
1 [69] isolated	19.26	5.087	0.0367
Coulomb potential	30.37	5.364	0.0047
DSK potential	29.47	5.321	0.0017
Dimer	29.49	5.321[b]	
2 [70] isolated	1.887	6.590	0.0030
Coulomb potential	1.808	6.557	0.0016
DSK potential	1.795	6.562	0.0010
Dimer	1.791	6.575[b]	
3 [71] isolated	4.983	6.422	0.0158
Coulomb potential	7.309	6.605	0.0059
DSK potential	7.004	6.588	0.0016
Dimer	6.840	6.588[b]	
4 [72] isolated	2.875	8.954	0.0134
Coulomb potential	3.505	8.828	0.0085
DSK potential	3.385	8.854	0.0019
Dimer	3.314	8.842[b]	
5 [73] isolated	4.941	7.939	0.0169
Coulomb potential	5.871	8.081	0.0101
DSK potential	5.622	8.052	0.0034
Dimer	5.473	8.057[b]	

[a] $\Delta q^{rms} = \sqrt{\frac{1}{N}\sum_{i=1}^{N}(q_i - q_i^{dimer})^2}$

[b] The distance between the centers of doublets, HOMO and LUMO are split within molecular pairs

the case of weak and medium-strong hydrogen bonds (H...O≥1.80 Å, H...N≥1.90 Å), but becomes inadequate for very short (and strong) hydrogen bonds.

Empirical correction: overall scaling

The AM1-derived dipole moments of dye molecules are smaller by 8 to 10% than the corresponding non-empirical (DFT/TZP and MP2/6-31G**) values. [22] Thus the overall scaling factor equal to 1.1 was applied to all point charges and dipoles when calculating the potential. On average, the INDO-CISD dipole moments are close to the non-empirical values; thus no overall correction was applied to the potential in the INDO-CISD calculations.

Empirical correction: C–H bond dipole moment

Since hydrogen atoms have only an *s* orbital within semiempirical methods, they are represented by atom-centered point charges. The AM1 Coulson charges on the hydrogen atoms in aromatic and aliphatic hydrocarbons are systematically too small, as compared to the charges extracted from the fitting of MEP. [38, 39, 40] The use of the AM1 Coulson charges placed at the hydrogen atom positions was found to provide reasonably accurate MEPs for molecules such as formamide, glycine zwitterion, uracil, etc. [41] However, these molecules are very polar; thus small contributions from the C–H bond dipoles are negligible. Dealing with aromatic hydrocarbons, a considerable improvement in the predicted crystal structures was obtained by placing atomic charges (q_H=−q_C=0.15e) in addition to the 6-exp atom–atom potential. [42]

There are many reasons to believe that weak hydrogen bonds involving the C–H groups play an important role for crystal formation and growth. [43] Therefore each hydrogen atom was assigned a point dipole oriented along the C–H bond direction. By fitting the MEP obtained from the AM1-calculated atomic charges, dipoles and quadrupoles to the MEP calculated at the MP2/6-311+G** level for six simple hydrocarbons (methane, ethylene, benzene, etc.), the value of the C–H correction dipole was estimated at 0.22 D.

Empirical correction: nitro and cyano groups

Semiempirical methods are known to systematically overestimate dipole moments of nitro compounds and underestimate dipole moments of nitriles. By fitting the AM1 dipole moments of 19 nitro compounds and 9 nitriles to the non-empirical values, the permanent correction factors of −1.16 and +1.15 D were determined for the NO_2 and CN groups, respectively. The following schemes of placing the compensation dipoles and charges were found to provide the best agreement between the semiempirical and ab initio (MP2/6-31G**) MEPs: for nitro compounds, the positive compensation charges on the oxygen atoms and the negative charge on the carbon atom the nitro group is attached to, and for nitriles, two equal compensation point dipoles on the carbon atom of the cyano group and the carbon atom this group is attached to. At the INDO-CISD level, the correction factors of −0.77 and +0.55 D were applied for the NO_2 and CN groups, respectively.

Results and discussion

The SCEP calculations were performed for 79 crystal structures; six of them contained two crystallographically independent, i.e. not related by symmetry, molecules. The atomic coordinates were taken from the original papers, except for those of the hydrogens, which were placed by assuming standard bond lengths and angles. Molecular diagrams of the compounds discussed below are shown in Fig. 7.

Ground-state molecular dipole moments

In most cases molecular dipole moments (μ) increase under the effect of SCEP, on the average by 37% for 79 species. The largest increase was observed for **1** (102%), **6A** (83%), and the orange polymorph of **7** (83%). The crystal field also changes the direction of molecular dipole moment. As shown in Fig. 8, the angle α subtended

Fig. 7 Molecular diagrams of the discussed compounds

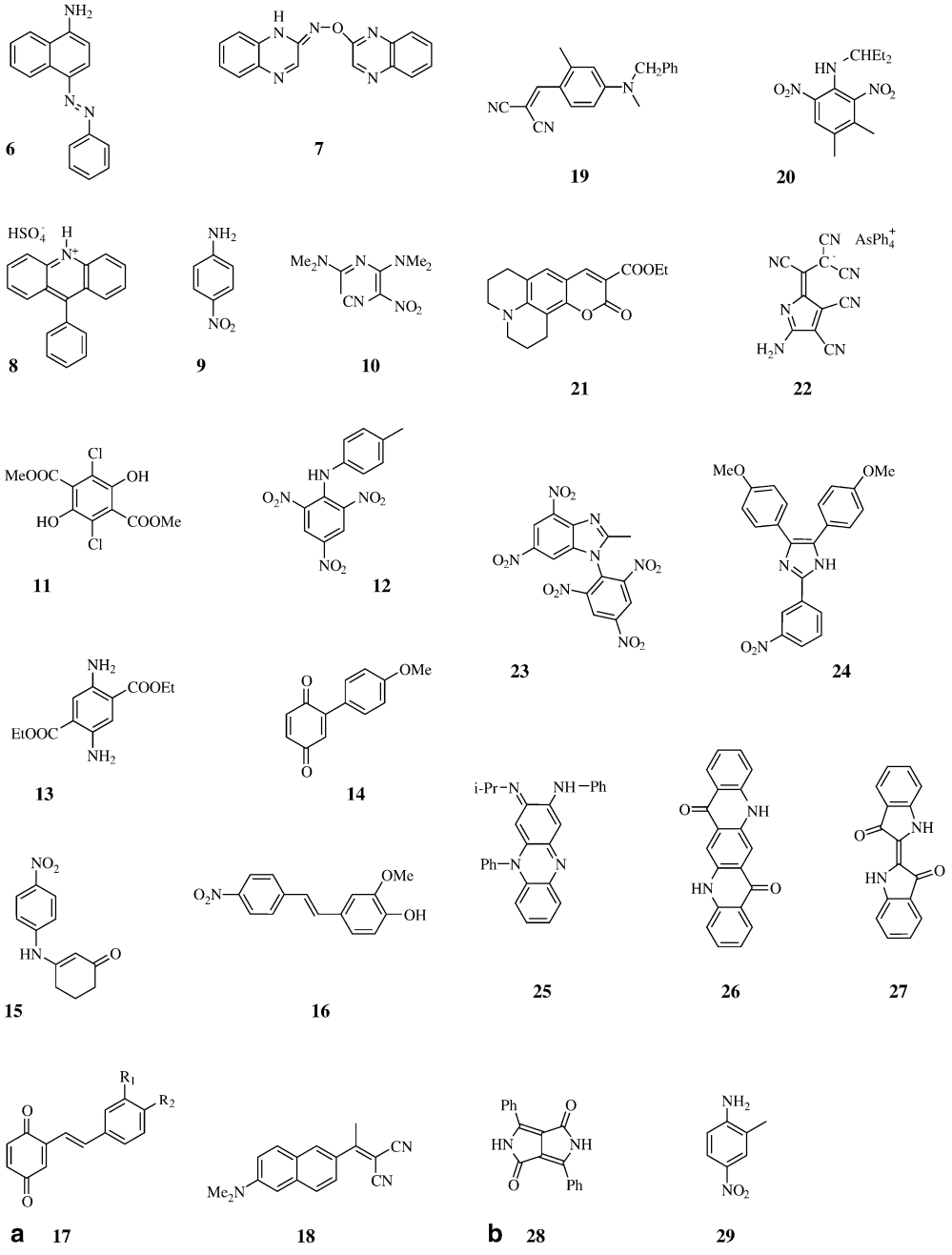

by vectors $\bar{\mu}_{isolated}$ and $\Delta\bar{\mu}=\bar{\mu}_{SCEP}-\bar{\mu}_{isolated}$ may be rather large, although its value tends to decrease with the increase in μ. This suggests that the mutual molecular arrangement in crystals is often not controlled by dipole–dipole interactions.

It is interesting to compare the effect of SCEP with the solvation effect modeled via the continuum approach, e.g., using the widespread COSMO method. [44] Within COSMO, the original set of atomic radii was retained (with the exception of nitrogen, for which the value of 1.80 Å [45] was used), and the value of an integer keyword called NSPA was set to 60. The values of dielectric permeability ε_{eq} were estimated in the course of COSMO calculations, providing the molecular dipole moments equal in magnitude to those obtained with SCEP. If the structure contains two or more independent molecules, each of them should be characterized by its own ε_{eq} value, since they have different crystal environments. For example, in structure **6** ε_{eq} for molecules A and B are $>\infty$ and 1.3, respectively.

All species studied were separated into groups corresponding to apolar ($1\leq\varepsilon_{eq}<4$), moderately polar ($4\leq\varepsilon_{eq}<10$) and strongly polar ($10\leq\varepsilon_{eq}<\infty$) solvents. For some molecules, the effect of SCEP cannot be modeled at any physically admissible value of ε_{eq}. The

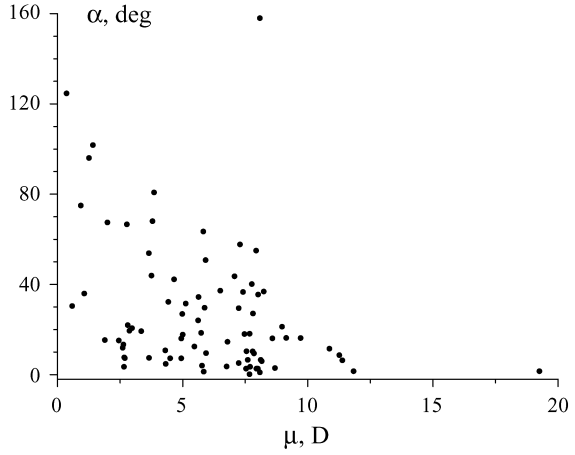

Fig. 8 Angles α subtended by vectors $\bar{\mu}_{isolated}$ and $\Delta\bar{\mu} = \bar{\mu}_{SCEP}-\bar{\mu}_{isolated}$ plotted against dipole moments of isolated molecules ($\mu_{isolated}$)

Table 2 Classification of molecules in their crystal environment by ε_{eq} calculated from molecular dipole moments (μ) and LUMO–HOMO energy gaps (ΔE)

	ε_{eq} from μ	ε_{eq} from ΔE
$\varepsilon_{eq}<1$	1	19
$1\le\varepsilon_{eq}<4$	18	15
$4\le\varepsilon_{eq}<10$	24	12
$10\le\varepsilon_{eq}<\infty$	15	8
$\varepsilon_{eq}>\infty$	15	26
Total number	73[a]	80

[a] Seven molecules are centrosymmetric

classification of crystal structures by ε_{eq} is given in Table 2.

Among 15 species of the "superpolar" group ($\varepsilon_{eq}>\infty$), seven are included in ionic structures, and only one ionic structure does not belong to this group (**8**, ε_{eq}=13.7). However, neither high molecular dipole moment, nor intermolecular hydrogen bonds guarantee a high ε_{eq} value. The correlation between ε_{eq} and $\mu_{isolated}$ is essentially absent (r=0.15), and the crystal structures with intermolecular hydrogen bonds are approximately uniformly distributed throughout all groups. Since polarity of the molecular crystal packing is not easily related to the packing motif, ε_{eq} may be used as an independent descriptor in the classification of crystal structures.

Energy gaps HOMO–LUMO

Many important photophysical and photochemical phenomena in molecular materials arise from electronic transitions between frontier orbitals; thus the HOMO–LUMO energy gap (ΔE) was used as another parameter which characterizes the whole molecule. The effect of SCEP on ΔE greatly differs from the solvent effect, and for many species these effects are opposite to each other. These results give an insight into the reasons for spectral distinctions between crystals of organic dyes and dye solutions. As shown in Table 2, for 55% of the species, the values of ε_{eq} lie outside the physically allowable range. For some molecules, the ε_{eq} values determined from dipole moments and ΔE agree well; however, in general the correlation between these parameters is very poor (r=0.27 for 26 molecules with $1<\varepsilon_{eq}<\infty$).

SCEP for molecular excitations

Many organic colorants show crystallochromy, i.e. the dependence of color on crystal packing. [46] This dependence has various reasons. Firstly, the molecules in the crystals may exist as different tautomers or may adopt different conformations. In this case, the difference in color can be explained by calculating the electronic spectra of these tautomers or conformers. Secondly, the absorption bands may be shifted and split due to the collective interactions within the crystals upon excitation. These effects can be considered at the level of the exciton–polariton approach. [47] Thirdly, the bands corresponding to intermolecular charge-transfer interactions can appear not only in the crystals with interlaced donor and acceptor molecules, but also in homomolecular crystals. [48] If intermolecular π interactions are strong, the excitonic and charge-transfer states mix and should be considered together within the general theory. [49] Finally, shifts of the absorption bands may arise from the perturbation of MOs under the effect of crystal environment, which is closely related in its nature to solvatochromism. Solvatochromic shifts are determined by three principal terms: orientational (permanent), inductive, and dispersion. [20, 50, 51] The Hamiltonian modification by SCEP simulates the orientational term, but the model presented in its current state does not account for the local inductive polarization of the crystal environment upon excitation of a molecule and the dispersion interaction, thus being a rather crude approximation. However, there are grounds to believe that, due to the long-range interactions in crystal lattices, the orientational term is the most packing-dependent one, whereas the two others do not change so drastically upon transfer from one type of molecular surrounding to another.

The mean unsigned $\Delta\nu=\nu_{SCEP}-\nu_{isolated}$ for 86 species is 1,560 cm^{-1}. The largest bathochromic shifts were calculated for some molecular complexes of **9** (from –5,200 to –4,900 cm^{-1}) and for **6A** (–3,670 cm^{-1}), the largest hypsochromic shifts were found for **1** (4,906 cm^{-1}) and for the orthorhombic polymorph of **10** (4,632 cm^{-1}).

The electrostatic fields in a crystal can also significantly modify the transition moment directions of some chromophores. [52] For example, under the effect of a crystal field the transition moments for the first and second $\pi\pi^*$ excitations of 9-ethylguanine undergo rotations of 22–31° and 17–21°, respectively. [9] Among the structures considered in this work, the 18° change of the

transition moment direction found for the orthorhombic polymorph of **10** is the largest; in most cases this value lies in the range from 2 to 8°. Only when the molecule has several closely spaced excited states dominated by the same set of electronic transitions, can large variations in the transition moments take place under the effect of SCEP, apparently as a result of their mixing. If the first excited state is well separated from the highest ones, as for the majority of dye molecules, SCEP does not cause any significant change in the transition moment.

It is noteworthy that semiempirical CI calculations often split the unique excited state of a molecule into a multiplet; thus the INDO/S results are to be monitored using experimental data or higher-level calculations (e.g., TD-DFT).

Crystallochromy: differently colored polymorphs

The first examples of differently colored crystalline forms of organic compounds were reported 95 years ago. [53] The current version of the Cambridge Structural Database [54] contains more than 50 families of differently colored polymorphs and pseudopolymorphs. Of practical significance are some pigment polymorphs that differ widely in their coloristic properties, e.g., perylene pigments whose solid state colors range from orange to black, while the color in solution always stays orange. [55]

The clear examples of conformational polymorphism and excitonic interactions were eliminated from consideration. Since INDO/S is not perfect in reproducing the spectra of sulfur-containing systems, all compounds of this type were also omitted. For six of 16 groups of polymorphs and pseudopolymorphs listed in Table 3 (**12**, **14**, **15**, **16**, **18**, **20**), the calculations employing SCEP provide a complete explanation of their difference in color with good agreement between experimental and calculated spectral shifts. For example, the long-wave edge of the absorption band in the red polymorph of **12** is shifted 2,200 cm^{-1} bathochromically with respect to the orange-yellow form, whereas the calculated shift is equal to 2,100 cm^{-1}. For **14**, experimental and calculated shifts are 1,340 cm^{-1} [56] and 1,900 cm^{-1}, respectively, and for **20** −1,460 and 1,550 cm^{-1}, respectively. Only the fluorescence emission spectra are available for **18** and **19**, and the difference between positions of the emission maxima is 1,500 and 1,230 cm^{-1}, respectively, versus 2,300 and 540 cm^{-1}, respectively, calculated with SCEP. In four cases (**13**, **17**, **19**, **25**) the effect of SCEP is not large enough, but after taking into account the differences in molecular geometry also insignificant by themselves, the calculated spectral shifts become large enough to explain the difference in color between polymorphs. For six remaining groups, SCEP does not provide the desired results, since the spectral shifts calculated for different polymorphs are almost equal. Nevertheless, in no case are the computational results in conflict with the experimental data.

Table 3 Differently colored polymorphs—INDO-CISD excitation energies (cm^{-1}), molecular diagrams are presented in Fig. 7

Compound	Polymorph	$\nu_{isolated}$	ν_{SCEP}	$\Delta\nu$
7 [13]	Orange	31,098	30,985	−113
	Yellow—mol. A	31,323	31,617	294
	Yellow—mol. B	31,322	31,007	−315
11 [74]	Yellow	25,076	25,186	110
	Light yellow	26,350	26,031	−319
12 [75]	Red	30,695	28,843	−1,852
	Orange-yellow	31,812	30,967	−845
13 [76]	Orange	24,951	24,205	−746
	Yellow	25,231	25,003	−228
14 [77]	Red	32,013	31,220	−793
	Yellow	32,734	33,118	+384
15 [78]	Orange	34,821	31,872	−2,949
	Yellow	34,935	32,573	−2,362
16 [79]	Red	32,492	31,791	−701
	Yellow	32,274	32,553	+179
17 [80], R_2=Cl	Dark red[a]	27,768	28,040	+272
R_1=R_2=H	Red	28,719	29,026	+307
R_1=R_2=CH_3	Red	29,821	29,394	−427
R_2=Cl	Red	30,713	29,624	−1,089
R_1=Cl	Light red	29,189	29,995	+806
18 [81]	Red	29,339	26,273	−3,066
	Yellow—mol. A	29,720	28,599	−1,121
	Yellow—mol. B	31,575	30,432	−1,143
19 [82]	Orange	29,423	28,456	−967
	Yellow—mol. A	28,430	28,998	+568
	Yellow—mol. B	30,885	30,015	−870
20 [83]	Orange	28,137	26,792	−1,345
	Yellow	27,706	28,346	+640
21	Orange [84]	29,565	27,826	−1,739
	Yellow [85]	29,385	27,505	−1,880
22	Purple [86]	19,865	19,135	−730
	Golden [87]	19,553	19,293	−260
23 [88]	Brown	32,497	32,442	−55
	Yellow	32,461	32,233	−228
24 [89]	Red—mol. A	28,314	27,765	−549
	Red—mol. B	29,541	29,036	−505
t-BuOH solvate	Orange	29,573	28,987	−586
C_6H_6 solvate	Intense yellow	29,446	28,823	−623
	Yellow [90]	30,923	30,245	−678
25 [91]	Red-orange	25,336	25,526	+190
DMF solvate	Red	25,242	25,022	−220

[a]All derivatives of **17** in acetone solution have λ_{max} at 418–420 nm

It is noteworthy that the spectral effects of SCEP for polymorphs **14** and **17** are rather large, though the molecular dipole moments are small.

Let us consider in detail the polymorphs **7** and **11**, which were studied earlier at various theoretical levels using the crystal field approach.

Three polymorphs are known for **11**: yellow, light yellow, and colorless. In the yellow crystal form, the molecules are almost planar, whereas in the light yellow and colorless polymorphs the OH and $COOCH_3$ groups are twisted out of the plane of the ring by about 40° and 70°, respectively. The 5,000 cm^{-1} difference in excitation

Table 4 Excitation energies (cm^{-1}) calculated with TD-DFT and various semiempirical methods for orange and light-yellow polymorphs of **7** (the latter contains two independent molecules, A and B, in a unit cell)

Method	Polymorph	$\nu_{isolated}$ [a]	ν_{SCEP} [a]	$\Delta\nu$
AM1, CI=(2,1)	Orange	33,035	39,579	6,544
	Yellow-A	33,636	43,678	10,042
	Yellow-B	34,378	35,368	990
AM1, CI=(4,2)	Orange	32,146	31,318	−828
	Yellow-A	32,458	33,329	871
	Yellow-B	32,961	32,912	−49
TD-DFT	Orange	26,797 [0.416]		
		29,100 [0.004]		
	Yellow-B	27,066 [0.409]		
		29,433 [0.003]		
AM1-CIS	Orange	27,668 [0.077]		
		29,832 [0.111]		
	Yellow-A	27,970 [0.082]		
		30,131 [0.106]		
	Yellow-B	28,253 [0.076]		
		30,084 [0.101]		
INDO-CISD	Orange	31,040 [0.654]	29,992 [0.403]	−1,048
		31,887 [0.050]	32,799 [0.241]	912
	Yellow-A	31,281 [0.601]	31,241 [0.435]	−40
		31,958 [0.041]	32,566 [0.180]	608
	Yellow-B	31,276 [0.590]	30,943 [0.639]	−333
		31,783 [0.060]	31,707 [0.060]	−76

[a] Oscillator strengths are given in square brackets

energy for colorless and yellow crystal forms was obtained at the HF/6-31+G* level [12] in very good agreement with the experimental [57] data. The data of Table 3 on the yellow and light yellow forms favor the viewpoint that their difference in color arises from conformational distinctions only, without any significant contribution from the crystal field.

The absorption band in the spectra of the orange polymorph of **7** is shifted bathochromically by 650 cm^{-1} with respect to the light yellow polymorph. [13] The effect of the crystal environment on excitation energy was modeled at the AM1 level using the single-transition approximation (STA), and the excitation energy of the orange form decreased by 1,000 cm^{-1} on inclusion of the crystal field in comparison with the light yellow form. [13] This level of consideration seems not to be correct for the two following reasons.

Firstly, STA presumes that excitation is dominated by the electron transition from the HOMO to the LUMO. This is not the case for molecule **7**. The two highest occupied and two lowest empty orbitals of this molecule result from the interaction of HOMOs and LUMOs of bicycles, and the mixing ratio is very sensitive to the molecular geometry and to external effects. The crystal field causes a radical change in the MO structure, hence for obtaining stable results all four frontier orbitals should be included in the CI procedure. The data in Table 4 demonstrate how strongly the results of calculations depend on the size of the configuration space.

Secondly, despite the fact that only one absorption band is present in the visible spectra of solutions and crystals of **7**, both semiempirical (AM1-CIS and INDO-CISD) and TD-DFT calculations predict two closely-spaced $\pi\pi^*$ transition in the visible area, although their relative intensities differ. Consequently, this splitting is an artifact, and the weighted average wavenumber for two lowest excitations (with squared transition moments as weighting factors) should be used for the analysis of crystallochromy. If only the first excitation is considered, the INDO-CISD results are close to the AM1 results with four-orbital configuration space. However, if average wavenumbers are compared (see Table 3), it becomes apparent that the difference in color cannot be ascribed to the effect of the crystal field.

It is likely that the colors of polymorphs of **7** are related to different packing arrangements. In crystals of the orange polymorph, the molecules form centrosymmetric dimers with overlapping bicycles and an interplanar separation of 3.42 Å; such a packing motif can favor the mixing of the intra- and intermolecular charge-transfer excitations. Similar packing features are absent from the crystals of the light yellow form.

Table 5 Hydrogen-bonded pigments **26**, **27**, and **28** (Fig. 7): calculated and experimental spectral shifts (cm^{-1}) and O...H distances

Pigment	Calculated	Observed	O...H (Å)
	$\nu_{isolated}-\nu_{SCEP}$	$\nu_{solution}-\nu_{solid}$	
26	1,475	1,500 [92]	1.81 [93]
27	1,120	1,310 [59]	2.11 [94]
28	70	−1,700, +1,520[a] [61]	1.83 [95]

[a] Absorption band split into doublet

Crystallochromy: hydrogen-bonded pigments

Industrial pigments **26**, **27**, and **28** show drastic difference in color between their crystals and solutions. In the

crystals, each molecule forms four medium-strong hydrogen bonds N–H...O to its closest neighbors; thus the observed crystallochromy is often ascribed to the effect of hydrogen bonds. [58, 59, 60] The results of INDO-CISD calculations for these compounds are given in Table 5. The effect of SCEP allows a rationalization of the crystallochromy for **26** and **27**, but not for **28**; since electronic excitation of this molecule is not accompanied by charge transfer from the NH to the carbonyl group, thus hydrogen bonds do not assist the excitation. The most likely reason for crystallochromy of **28** and its derivatives are excitonic effects, as proposed by Mizuguchi. [61]

On intermolecular resonance-assisted hydrogen bonding

If the π-system delocalization gives rise to charge transfer from the hydrogen-bond donor atom to the acceptor atom, thus triggering a synergistic mechanism between hydrogen-bond strengthening and resonance reinforcement; such a system is referred to as resonance-assisted hydrogen bonding. [62, 63] Among the structures considered in this study, 18 belong to this class. They demonstrate diverse H-bonding patterns: centrosymmetric dimers and infinite 1D, 2D and 3D aggregates.

In order to separate the effect of hydrogen bonding from the total effect of SCEP, SCF calculations with the potential produced by only hydrogen-bonded molecules were carried out. Under the effect of this potential, the molecular dipole moments changed by $\Delta_1=\mu_{\text{H-bonded}}-\bar{\mu}_{\text{isolated}}$, and further by $\Delta_2=\mu_{\text{SCEP}}-\bar{\mu}_{\text{H-bonded}}$ after the rest of the crystal structure was taken into consideration. For 18 species, Δ_1 ranged from 0.63 to 3.33 D and the ratio Δ_1/Δ_2 was 1.1 on average. For two species only, SCEP was dominated by contributions from the H-bonded molecules ($\Delta_1>5\Delta_2$), and in seven cases Δ_2 was larger than Δ_1. In other words, inclusion of the long-range electrostatic interactions is required when modeling the H-bonded crystals.

As an example let us compare the structures of *p*-nitroaniline (**9** [64]), its simple derivative (**29** [65]), and their molecular complexes. Molecular dipole moments of isolated **9** and **29** range in these structures from 7.6 to 8.1 D (small variations in μ arise from subtle distinctions in bond dimensions). In crystals, the dipole moment of **9** increases by almost 3 D under the effect of four H-bonded neighbors, and slightly decreases after all other molecules are taken into account; thus the total effect of SCEP is 2.7 D. The largest $\Delta\mu$ of 3.3 D is calculated for the structure of the molecular complex of **9** with 18-crown-6, [66] although the hydrogen bonds in this compound are not resonance assisted. As in pure **9**, in crystals of **29** each molecule has four hydrogen-bonded neighbors, and under their influence the molecular dipole moment increases by 3 D. However, the effect of the rest of the crystal structure exceeds the effect of hydrogen bonding and is directed oppositely to it; thus the total effect of SCEP decreases the molecular dipole moment by 1.15 D.

Conclusions

Exploring molecular crystal structures, crystallographers traditionally employ a geometric approach, which is based on recognition of the short-contact patterns, i.e. ribbons, stacks, layers, rings, 3D networks etc. For example, a special nomenclature has been proposed for the graph set analysis of hydrogen bonds. [67, 68] However, such an analysis does not provide any information about the strength of intermolecular interactions and their effect on electronic and spatial molecular structure within a crystal.

The calculations employing SCEP allow rationalization of differences between the molecules in a crystal and these molecules in solution or the gas phase. The effect of crystal packing is often quite different from the solvent effect modeled at the level of the dielectric continuum approach. The most probable reason for this difference is that the continuum approach assumes that at any point on the dielectric surface the induced charge is an exact function of the molecular electrostatic potential, whereas the SCEP approach is based on real crystal packing; thus it does not ensure that any charge is surrounded by corresponding opposite charges. The effect of SCEP is subject to wide variations depending on the packing motif, thus illuminating the distinctions between polymorphs. Due to this effect, crystallographically independent molecules differ in their electronic structure.

Acknowledgements The author wishes to thank Dr. K.A. Paseshnichenko for her assistance with the manuscript. The license fee for Cambridge Database was covered by the Russian Foundation for Fundamental Research (grant no. 99-07-90133).

References

1. Sheats JR, Barbara PF (1999) Acc Chem Res 32:191–192
2. Dovesi R, Causa M, Orlando R, Roetti C, Saunders VR (1990) J Chem Phys 92:7402–7411
3. Winkler B (1999) Z Kristallogr 214:506–527
4. Almlöf J, Wahlgren U (1973) Theor Chim Acta 28:161–168
5. Saebø S, Klewe B, Samdal S (1983) Chem Phys Lett 97:499–502
6. Ángyán JG, Silvi B (1987) J Chem Phys 86:6957–6966
7. Krijn MPCM, Feil D (1988) J Chem Phys 89:4199–4208
8. Popelier P, Lenstra AT, van Alsenoy C, Geise HJ (1989) J Am Chem Soc 111:5658–5660
9. Theiste D, Callis PR, Woody RW (1991) J Am Chem Soc 113:3260–3267
10. Lenstra ATH, van Alsenoy C, Verhulst K, Geise HJ (1994) Acta Crystallogr Sect B 50:96–106
11. Franckaerts K, Peeters A, Lenstra ATH, van Alsenoy C (1997) Electron J Theor Chem 2:168–179
12. Peeters A, Lenstra ATH, van Doren VE, van Alsenoy C (2001) J Mol Struct (Theochem) 546:25–32
13. Csikós É, Ferenczy GG, Ángyán JG, Böcskei Z, Simon K, Gönczi C, Hermecz I (1999) Eur J Org Chem 2119–2125
14. Woody RW, Raabe G, Fleischhauer J (1999) J Phys Chem B 103:8984–8991
15. Ferenczy GG, Párkányi L, Ángyán JG, Kálmán A, Hegedüs B (2000) J Mol Struct (Theochem) 503:73–79
16. ADF Program System (2000) Release 2000.02. ADF User's Guide, pp 65–66
17. Mestechkin MM (1997) J Phys:Condens Matter 9:157–164

18. Miertuš S, Tomasi J (1982) Chem Phys 65:239–245
19. Wang B, Ford GP (1992) J Chem Phys 97:4162–4169
20. Rauhut G, Clark T, Steinke T (1993) J Am Chem Soc 115:9174–9181
21. Yatsenko AV, Paseshnichenko KA (2000) Chem Phys 262:293–301
22. Yatsenko AV, Paseshnichenko KA (2001) J Mol Model 7:384–391
23. Stewart JJP (1993) MOPAC 7 program package, QCPE No 455
24. Dewar MJS, Zoebisch EG, Healy EF, Stewart JJP (1985) J Am Chem Soc 107:3902–3909
25. Stewart JJP (1989) J Comput Chem 10:209–220
26. Dick B, Hohlneicher G (1979) Theor Chim Acta 53:221–251
27. Dick B, Nickel B (1983) Chem Phys 78:1–16
28. Pariser R, Parr RG (1953) J Chem Phys 21:767–776
29. Bauernschmitt R, Ahlrichs R (1996) Chem Phys Lett 256:454–464
30. Frisch MJ, Trucks GW, Schlegel HB, Scuseria GE, Robb MA, Cheeseman JR, Zakrzewski VG, Montgomery JA, Jr., Stratmann RE, Burant JC, Dapprich S, Millam JM, Daniels AD, Kudin KN, Strain MC, Farkas O, Tomasi J, Barone V, Cossi M, Cammi R, Mennucci B, Pomelli C, Adamo C, Clifford S, Ochterski J, Petersson GA, Ayala PY, Cui Q, K. Morokuma K, Malick DK, Rabuck AD, Raghavachari K, Foresman JB, Cioslowski J, Ortiz JV, Baboul AG, Stefanov BB, Liu G, Liashenko A, Piskorz P, Komaromi I, Gomperts R, Martin RL, Fox DJ, Keith T, Al-Laham MA, Peng CY, Nanayakkara A, Gonzalez C, Challacombe M, Gill PMW, Johnson B, Chen W, Wong MW, Andres JL, Gonzalez C, Head-Gordon M, Replogle ES, Pople JA (1998) Gaussian 98, revision A 7. Gaussian, Pittsburgh, Pa.
31. Becke AD (1993) J Chem Phys 98:5648–5652
32. Lee C, Yang W, Parr RG (1988) Phys Rev B 37:785–789
33. Guillaumont D, Nakamura S (2000) Dyes Pigm 46:85–92
34. HyperChem (Release 4) (1994) Hypercube
35. Dewar MJS, Thiel W (1977) Theor Chim Acta 46:89–104
36. Dewar MJS, Sabelli NL (1962) J Phys Chem 66:2310–2316
37. Klopman G (1964) J Am Chem Soc 86:4550–4557
38. Besler BH, Merz KM, Kollman PA (1990) J Comput Chem 11:431–439
39. Chirlian LE, Francl MM (1987) J Comput Chem 8:894–905
40. Wang B, Ford GP (1994) J Comput Chem 15:200–207
41. Rauhut G, Clark T (1993) J Comput Chem 14:503–509
42. Williams DE, Starr TL (1977) Comput Chem 1:173–177
43. Steiner T (1996) Crystallogr Rev 6:1–57
44. Klamt A, Schüürmann G (1993) J Chem Soc Perkin Trans 2:799–805
45. Yatsenko AV, Paseshnichenko KA (1999) J Mol Struct (Theochem) 492:277–283
46. Klebe B, Graser F, Hädicke E, Berndt J (1989) Acta Crystallogr Sect B 45:69–77
47. Philpott MR (1971) J Chem Phys 54:2120–2129
48. Sebastian L, Weiser G, Bässler H (1981) Chem Phys 61:125–135
49. Hoffmann M, Schmidt K, Hasche T, Agranovich VM, Leo K (2000) Chem Phys 258:73-96
50. Cramer CJ, Truhlar DG (1999) Chem Rev 99:2161–2200
51. Li J, Cramer CJ, Truhlar DG (2000) Int J Quantum Chem 77:264–280
52. Woody RW, Raabe G, Fleischhauer J (1999) J Phys Chem B 103:8984–8991
53. Hantzch A (1907) Z Angew Chem 20:1889–1889
54. Allen FH, Kennard O (1993) Chem Des Autom News 8:31–37
55. Hunger K (1999) Rev Prog Coloration 29:71–84
56. Aihara J, Kushibiki G, Matsunaga Y (1973) Bull Chem Soc Jpn 46:3584–3585
57. Curtin DY, Byrn SR (1969) J Am Chem Soc 91:6102–6106
58. Adachi M, Nakamura S (1994) J Phys Chem 98:1796–1801
59. Miehe G, Süsse P, Kupcik V, Egert E, Nieger M, Kunz G, Gerke R, Knieriem B, Niemeyer M, Lüttke W (1991) Angew Chem Int Ed Engl 30:964–967
60. Linke G (2000) Dyes Pigm 44:101–122
61. Mizuguchi J (2000) J Phys Chem 104:1817–1821
62. Gilli G, Bellucci F, Ferretti V, Bertolasi V (1989) J Am Chem Soc 111:1023–1028
63. Bertolasi V, Nanni L, Gilli P, Ferretti V, Gilli G, Issa YM, Sherif OE (1994) New J Chem 18:251–261
64. Tonogaki M, Kawata T, Ohba S, Iwata Y, Shibuya I (1993) Acta Crystallogr Sect B 49:1031–1039
65. Ferguson G, Glidewell C, Low JN, Skakle JMS, Wardell JL (2001) Acta Crystallogr Sect C 57:315-316
66. Weber G (1981) Z Naturforsch B 36:896–897
67. Etter MC (1990) Acc Chem Res 23:120–126
68. Bernstein J, Davis RE, Shimoni L, Chang NL (1995) Angew Chem Int Ed Engl 34:1555–1573
69. De Ridder DAJ, Heijdenrijk D, Schenk H, Dommisse RA, Lemiere GL, Lepoivre JA, Alderweireldt FA (1990) Acta Crystallogr Sect C 46:2197–2199
70. Yatsenko AV, Tafeenko VA, Zhukov SG, Medvedev SV, Popov SI (1995) Z Kristallogr 210:969–970
71. Yatsenko AV, Tafeenko VA, Zhukov SG, Medvedev SV, Popov SI (1997) Struct Chem 8:197–204
72. Kvick A, Thomas R, Koetzle TF (1976) Acta Crystallogr Sect B 32:224–231
73. Doyle AA, Parsons S, Solan GA, Winpenny REP (1997) J Chem Soc Dalton Trans 2131-2137
74. Yang QC, Richardson MF, Dunitz JD (1989) Acta Crystallogr Sect B 45:312–323
75. Yatsenko AV, Tafeenko VA, Mikhalev OV, Il'ina IG, Aslanov LA (1997) XVII European Crystallographic Meeting, Lisbon, Book of Abstracts, p 105
76. Mann BJ, Duesler EN, Paul IC, Curtin DY (1981) J Chem Soc Perkin Trans 2:1577–1582
77. Desiraju GR, Paul IC, Curtin DY (1977) J Am Chem Soc 99:1594–1601
78. Huang K-S, Britton D, Etter MC, Byrn SR (1996) J Mater Chem 6:123–129
79. Gleixner A, Hiller J, Debaerdemaeker T, Lentz A, Walz L (1998) Z Kristallogr 213:411–415
80. Irngartinger H, Stadler B (1998) Eur J Org Chem 605–626
81. Jacobson A, Petric A, Hogenkamp D, Sinur A, Barrio JR (1996) J Am Chem Soc 118:5572–5579
82. Abe J, Shirai Y, Sakai K, Tsubomura T (1995) J Phys Chem 99:8108–8120
83. Stockton GW, Godfrey R, Hitchcock P, Mendelsohn R, Mowery PC, Rajan S, Walker AF (1998) J Chem Soc Perkin Trans 2:2061–2071
84. Honda T, Fujii I, Hirayama N, Aoyama N, Miike A (1996) Acta Crystallogr Sect C 52:395–397
85. Yip B-C, Fun H-K, Sivakumar K, Zhou Z-Y (1995) Acta Crystallogr Sect C 51:956–958
86. Dessy G, Fares V, Flamini A, Giuliani AM (1985) Angew Chem 97:433–434
87. Fares V, Flamini A, Poli N (1995) J Chem Res Synopsis 228–229
88. Freyer AJ, Lowe-Ma CK, Nissan RA, Wilson WS (1992) Austr J Chem 45:525–539
89. Inouye Y, Sakaino Y (2000) Acta Crystallogr Sect C 56:884–887
90. Inouye Y, Shimokoshi S, Sakaino Y (1999) Acta Crystallogr Sect C 55:2084–2087
91. Rychlewska U, Broom MBH, Eggleston DS, Hodgson DJ (1985) J Am Chem Soc 107:4768–4772
92. Kalinowski J, Stampor W, DiMarco P, Fattori V (1994) Chem Phys 182:341–352
93. Potts GD, Jones W, Bullock JF, Andrews SJ, Maginn SJ (1994) J Chem Soc Chem Commun 2565–2566
94. Süsse P, Steins M, Kupcik V (1988) Z Kristallogr 184:269–273
95. Mizuguchi J, Wooden G (1991) Ber Bunsenges Phys Chem 95:1264–1274